Tree-ring based annual precipitation reconstruction for the southern Three-River Headwaters region, China

Dingmu Xiao, Xiaomei Huang and Ningsheng Qin

ABSTRACT

Tree-ring width standard chronologies were created from *Juniperus przewalskii* Kom data collected in the southern Three-River Headwaters (TRH) region. Statistical analysis results showed high correlation between the first primary component (PC1) of the four chronologies and instrumental precipitation records during the annual September–August interval. Precipitation of the region was reconstructed for the past 461 years. It was verified that the reconstruction model was stable by split-sample calibration-verification statistics. The reconstruction series revealed 22 extremely dry years and 9 extremely wet years. Results showed relatively dry periods occurred during 1567–1597, 1604–1614, 1641–1656, 1684–1700, 1734–1755, 1817–1830, 1913–1932, 1953–1971, 1990–2005. Relatively wet periods occurred during 1615–1630, 1657–1683, 1701–1733, 1756–1786, 1798–1816, 1844–1855, 1864–1875, 1885–1912, 1933–1952, 1977–1989. Comparison with tree-ring based precipitation reconstructions, and chronologies from surrounding areas provided a high degree of confidence in our reconstruction, and correlated well with the Monsoon Asia Drought Atlas (MADA) dataset in the public section of corresponding grids. The empirical mode decomposition analysis suggests the existence of significant periods with intervals of 2–5, 6–10, 11–18, and 28–60 years. This research contributes to a better understanding of historical variations in precipitation and will aid in future plans to address climate change of the TRH region.

Key words | dendroclimatic, precipitation reconstruction, Tibetan Plateau, tree-ring width

Dingmu Xiao (corresponding author)
Xiaomei Huang
Chengdu Institute of Plateau Meteorology,
China Meteorological Administration,
Chengdu 610072,
China
E-mail: *noonemao520@163.com*

Ningsheng Qin
Climate Center of Sichuan Province,
Chengdu 610072,
China

INTRODUCTION

The Three-River Headwaters (TRH) region (31°39′–36°16′N, 89°24′–102°23′E) is in the hinterland of the Tibetan Plateau (Liu *et al.* 2005). The TRH region is the source of the Yangtze, Yellow, and Lancang rivers. This important region of the Tibetan Plateau has provided large amounts of water resources for most Asian countries (such as China, Myanmar, Laos, Thailand, Kampuchea, Vietnam, etc.). Thus, climate change relating to runoff has important influences on the social and economic development of this region. In recent decades, the impact of climate change has progressively been causing deterioration of the ecological environment of the region which has resulted in drought or floods, crop failure and famine, and changes in the hydrological regimes of monsoonal Asia (Zhao & Zhou 2005; Harris 2010; Shao *et al.* 2010a, 2010b; Wu *et al.* 2011). Understanding long-term precipitation variability in the region is important because precipitation and the availability of water resources in the region are critical for both the present and the future of the TRH region. However, meteorological stations were not installed in this area until the 1950s, which limits the analysis of long-term climate trends. This situation could be greatly improved by using a dendroclimatology method. Due to the accurately dated, continuous, high-resolution, precisely measured ring widths, and sensitive relations to climate, tree rings play an important role in reconstructing past environmental

doi: 10.2166/wcc.2018.190

and climatic changes over the past millennium on regional, hemispheric, and even global scales.

Numerous dendroclimatology studies have been conducted in the TRH region (Sheppard *et al.* 2004; Shao *et al.* 2005, 2010c; Liu *et al.* 2006a, 2006b; Gou *et al.* 2007a, 2007b, 2008; Li *et al.* 2008; Wang *et al.* 2008; Fan *et al.* 2008, 2009; Gou *et al.* 2010, 2014a, 2014b; Yang *et al.* 2014), and improved our understanding about climate change over the past century or even longer in the TRH region. However, considering the immense size of the TRH region, the geographical distribution of the dendroclimatic records is insufficient, and only a few of them were related to variations in precipitation or drought in the southern TRH region (Wang *et al.* 2008; Fang *et al.* 2010a, 2010b). Previous studies have provided valuable insights on climate in the past. However, there have been few tree-ring based reconstructions of regional precipitation for the southern TRH region, and numbers of tree-ring chronologies have been very small. Also, only one or two meteorological stations are used in these studies, and the inclusion of more stations in the average meteorological records would represent broader regional climatic conditions. Therefore, we used the averaged dataset of the four stations. The Empirical Mode Decomposition (EMD) method (Huang *et al.* 1998) was employed to extract multi-scale variability of the reconstructed precipitation, and may provide more comprehensive understanding of the differing time scales for intrinsic climate signals in our study. In the present work, we combine four moisture-sensitive tree-ring width chronologies archived in this area to extract the regional climate signals, and reconstruct a 461-year annual precipitation of the southern TRH region. Furthermore, we explore the commonalities in regional precipitation of the past.

MATERIALS AND METHODS

Study area description and meteorological data

The southern TRH region is located in the east-central area of the Tibetan Plateau (Figure 1). This region is arid with a plateau-continental climate (He 2008). Its climate is affected by the South Asian and the East Asian monsoon. The annual mean temperature is −2.42°C–2.87°C and annual rainfall is 490–680 mm (1951–2006) (He 2008). The tree species used in this study is *Juniperus przewalskii* Kom., a conifer with a long life span (Zhou *et al.* 1986).

The meteorological data used in this study are monthly total precipitation and monthly mean temperature from Qumalai, Zhiduo, Zaduo, Qingshuihe, and Yushu meteorological stations (Figure 1 and Table 1). We used these stations because they are the nearest meteorological stations. The climate of the southern TRH region is characterized by mild, wet summers and cold, dry winters (Figure 2). The precipitation distribution has a clear summer maximum reflecting the effect of the Asian summer monsoon. To confirm the coherency of the meteorological data we have also checked for the significant correlations among the five stations for each month (Table 2). For the reason of effectively reducing the small-scale noise or stochastic components contained in a single station and represent broader regional climatic conditions (Davi *et al.* 2006; Bao *et al.* 2015), we used the arithmetical averaged dataset of the five stations for our analyses.

Tree-ring width chronology development

The four sampling sites are located in the southern TRH region: Angsai village site (AS), located in Zaduo, Qinghai Province, China; Xiarishi village site (XRS), located in Zhiduo, Qinghai Province, China; Yuegai village site (YG), located in Qumalai, Qinghai Province, China; and Bagan village site (BG), located in Qumalai, Qinghai Province, China (Figure 1 and Table 1). Tree-ring samples were collected from healthy juniper trees. Most samples were taken from isolated trees or trees in small groves to reduce the effects of competition on tree growth by neighboring trees. One hundred and eight trees were collected in this study. All tree-ring samples were taken back to the tree-ring lab. After mounting and sanding, the annual widths of cores were measured with a LINTAB tree-ring measurement station at 0.001 mm precision. The quality of cross-dating was examined with the computer software COFECHA (Holmes 1983; Cook & Kairiukstis 1990; Fritts 2001). There are very few missing rings in the samples. Therefore, a missing ring in other samples could be determined by comparing the skeleton-plotting and ring width series plotting with the

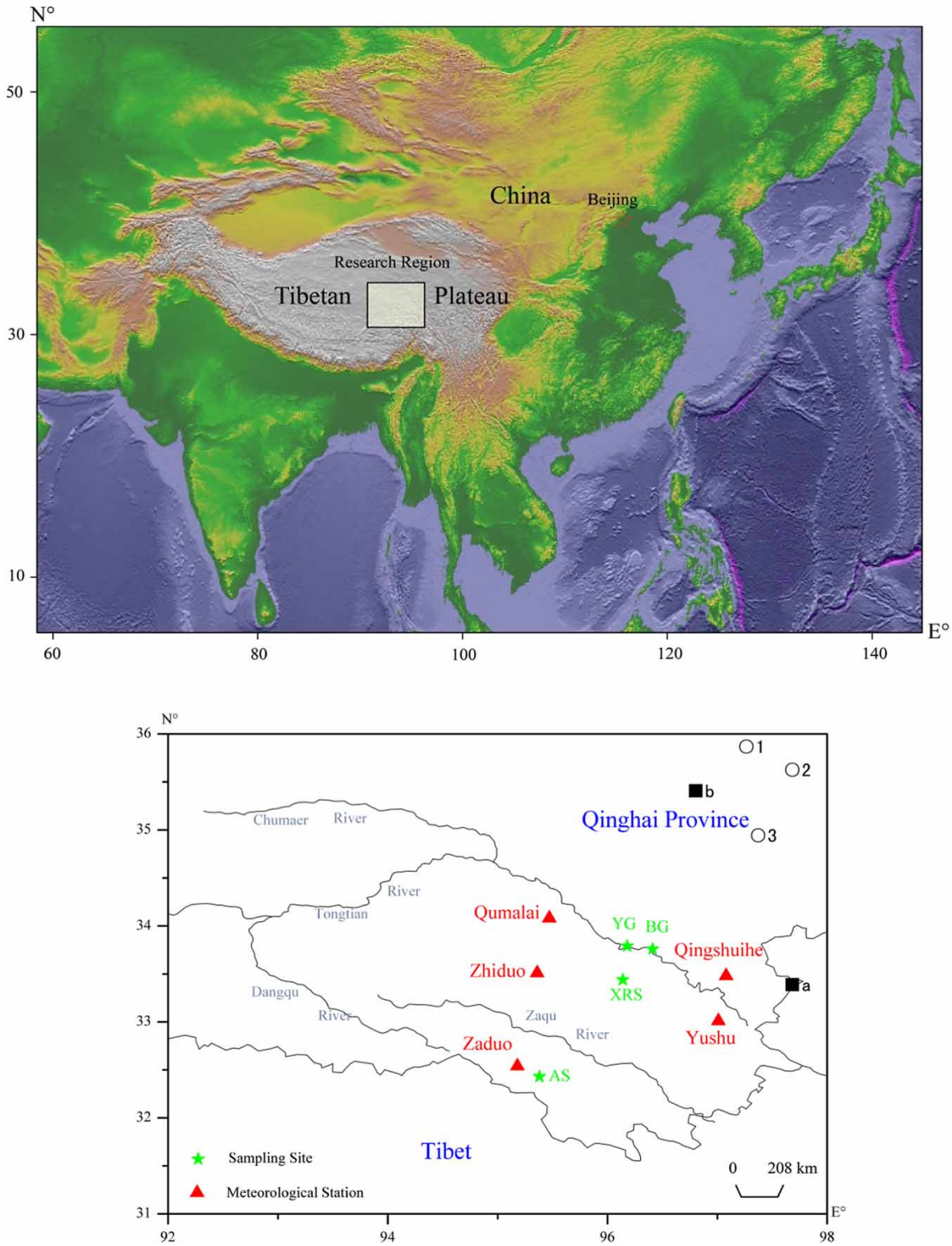

Figure 1 | Map showing the tree-ring sampling sites and the meteorological stations. 1, 2, and 3 denote the tree-ring chronologies from Delingha, Wulan, and Shenge, respectively. a and b denote the southeastern Tibetan Plateau (Fang *et al.* 2010a, 2010b), and the northeastern Tibetan Plateau (Yang *et al.* 2014), respectively.

Table 1 | Details of the tree-ring sampling sites and the meteorological stations

Date type	Site code	Location (latitude; longitude)	Elevation (m)	Time interval
Tree ring	AS	32°43′ N, 95°38′ E	3,992–4,092	1474–2013
	XRS	33°44′ N, 96°14′ E	3,908–4,050	1553–2013
	YG	33°79′ N, 96°18′ E	4,355–4,455	1066–2013
	BG	33°76′ N, 96°41′ E	3,933–4,233	1299–2013
Meteorological data	Qumalai	34°08′ N, 95°47′ E	4,175	1968–2013
	Zhiduo	33°51′ N, 95°36′ E	4,181	1968–2013
	Zaduo	32°54′ N, 95°18′ E	4,066	1968–2013
	Qingshuihe	33°48′ N, 97°08′ E	4,415	1968–2013
	Yushu	33°01′ N, 97°01′ E	3,681	1968–2013

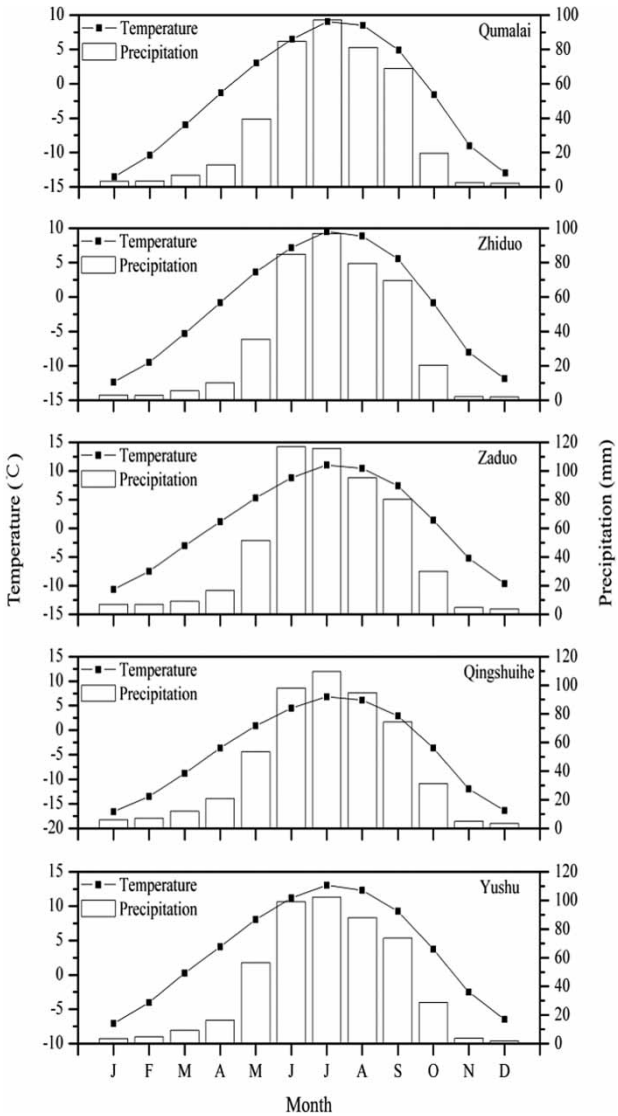

Figure 2 | Plot showing the distribution of monthly average precipitation and temperature (1968–2013) of the five meteorological stations (Qumalai, Zhiduo, Zaduo, Qingshuihe, and Yushu).

samples from younger trees. To retain more climate signal, each tree-ring series was detrended conservatively by fitting negative exponential curves. Finally, the detrended tree-ring series were used to develop the standard (STD), residual (RES), and arstan (ARS) chronologies with the computer software ARSTAN (Fritts 1976; Cook 1985; Fang *et al.* 2010a, 2010b) In this study, we used the STD chronology, which preserves more climate signals (Table 3). Figure 3 shows the chronology and sample depth (number of core/tree) of the four sampling sites. Due to sample size decreases in the early phase of the chronology, the expressed population signal (EPS > 0.85) was used to evaluate reliability of the tree-ring width chronology (Wigley *et al.* 1984). Figure 3 also demonstrates that the variations of the four chronologies are highly similar to

Table 2 | Correlation coefficients of meteorological stations[a] (1968–2013)

Site code	Qumalai	Zhiduo	Zaduo	Qingshuihe	Yushu
Temperature					
Qumalai	–	–	–	–	–
Zhiduo	1	–	–	–	–
Zaduo	0.99	0.99	–	–	–
Qingshuihe	1	1	0.99	–	–
Yushu	0.99	0.99	0.99	0.99	–
Precipitation					
Qumalai	–	–	–	–	–
Zhiduo	0.99	–	–	–	–
Zaduo	0.99	0.99	–	–	–
Qingshuihe	0.99	0.99	0.99	–	–
Yushu	0.99	0.99	0.99	0.99	–

[a]Correlation coefficients are at the 0.01 confidence level.

Table 3 | Statistics of standard chronologies

Statistical characteristics	AS	XRS	YG	BG
Species	*Juniperus przewalskii* Kom	*Juniperus przewalskii* Kom	*Juniperus przewalskii* Kom	*Juniperus przewalskii* Kom
Number (core/tree)	56/28	53/26	55/27	54/27
Expressed population signal (EPS) >0.85	1639–2013	1602–2012	1395–2013	1500–2013
Mean sensitivity	0.28	0.21	0.19	0.34
Mean correlations among all radii	0.41	0.43	0.36	0.34
Mean correlations between trees	0.42	0.44	0.37	0.36
Mean correlations within trees	0.61	0.80	0.69	0.72
Signal-to-noise ratio	26.19	22.12	20.16	21.91
Expressed population signal	0.96	0.96	0.95	0.96
Variance 1st eigenvector	47.90%	42.90%	38.70%	47.20%

each other. Table 4 shows the correlation coefficients between the chronologies. These high correlations indicate that tree growth at these four sites is limited by a similar set of environmental factors, most likely related to climate. Accordingly, we decided to use a principal components analysis (PCA) to combine the chronologies into a single predictor variable. The PCA of the ARSTAN chronologies resulted in the first principal component (PC1) with an eigenvalue more than one that explained 84.5% of the variance. For subsequent dendroclimatic analyses, we used PC1 as the primary predictor variables. The reliable portion of the four tree-ring chronologies extended from 1553 to 2013 (461 years).

Methods

Correlation analysis was applied to identify the relationship between tree-ring growth and climate factors. Linear regression analysis was utilized to reconstruct the precipitation. To understand the low-frequency variability of the reconstruction, the reconstructed series was subjected to the 10-year fast Fourier transformation (FFT). FFT is an algorithm that samples a signal over a period of time (or space) and divides it into its frequency components. These components are single sinusoidal oscillations at distinct frequencies, each with their own amplitude and phase (Van Loan 1992). EMD (Huang *et al.* 1998) is a useful method for the analysis of non-stationary and non-linear data. It can decompose any complicated data into finite and often a small number of intrinsic mode functions (IMF). The EMD was used to estimate the periods in the precipitation record.

RESULTS

Tree rings' response to climate

The PC1 of the four chronologies were significantly and negatively correlated with temperature and significantly and positively correlated with precipitation (Figure 4). The PC1 of the four chronologies correlate positively with precipitation of the previous September–October, the current April–May, and the current July–August, but negatively with temperature of the current February, May, and July.

Reconstruction of precipitation

Based on the above climate correlation analysis results, we concluded that total September–August precipitation is the most appropriate seasonal predictand for developing a climate reconstruction from the tree-ring width time series.

A linear regression model between the PC1 of the four chronologies and precipitation was established as follows:

$$P = 476.31 + 87.77PC \ (R^2 = 0.381) \quad (1)$$

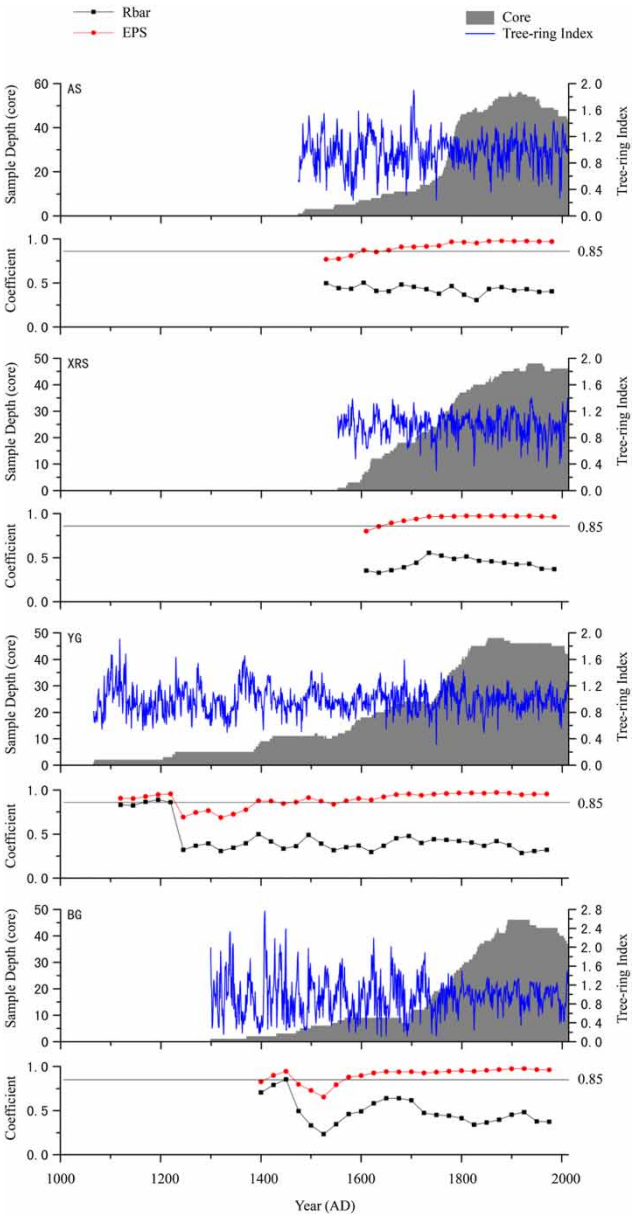

Figure 3 | Plot of the standard chronologies and sample depth.

Table 4 | Correlation coefficients of chronologies[a]

Site code	AS	XRS	YG	BG
AS	1			
XRS	0.67	1		
YG	0.65	0.62	1	
BG	0.62	0.63	0.64	1

[a]Correlation coefficients are significant at the 0.01 confidence level.

P represents annual precipitation from previous September to current August, and PC represents the PC1 of the four chronologies.

During the 1969–2013 calibration period, the reconstruction explained 38.1% of the variance (36.6% after adjustment for loss of degrees of freedom). Split-sample calibration-verification test results (Table 5) show high correlation coefficients in both calibration and verification periods (Meko & Graybill 1995). Results of the split calibration-verification test showed that the values of reduction of error (RE) and coefficient of efficiency (CE) were positive. The results of the sign test (ST) were significant at the 0.01 level. The transfer model therefore successfully reconstructed the annual precipitation over the 1553–2013 period. We compared the reconstructed precipitation with the meteorological measurement data in order to verify the reliability of the reconstruction results. The comparison indicates close agreement between the meteorological measurement and the reconstructed series (Figure 5).

The reconstructed total precipitation from previous September to current August for the southern TRH region is presented in Figure 6. The mean value and standard deviation (SD) of the reconstructed precipitation for the period 1553–2013 were 476.31 mm and 33.14 mm, respectively.

We defined a wet year as more than +1 SD and a dry year as less than −1 SD. Extremely wet years were defined by values above +2 SD and extremely dry years had values below −2 SD (Li *et al.* 2007; Chen *et al.* 2015). Under these definitions, 71 dry years and 65 wet years occurred during the entire period. There were 22 extremely dry years and 9 extremely wet years (Table 6). As shown in Table 6, there were 9 extremely dry years in the 17th century, 4 extremely dry years in the 18th century, 2 extremely dry years in the 19th century, and 4 extremely dry years in the 20th century. This indicated that more extreme single-year droughts occurred in the 17th, 18th, and 20th centuries than 19th century in the southern TRH region. The wettest year is 1624 (590.00 mm) and the driest year is 1749 (355.92 mm).

Wet periods (lasted longer than 11 years) were 1615–1630, 1657–1683, 1701–1733, 1756–1786, 1798–1816, 1844–1855, 1864–1875, 1885–1912, 1933–1952, and

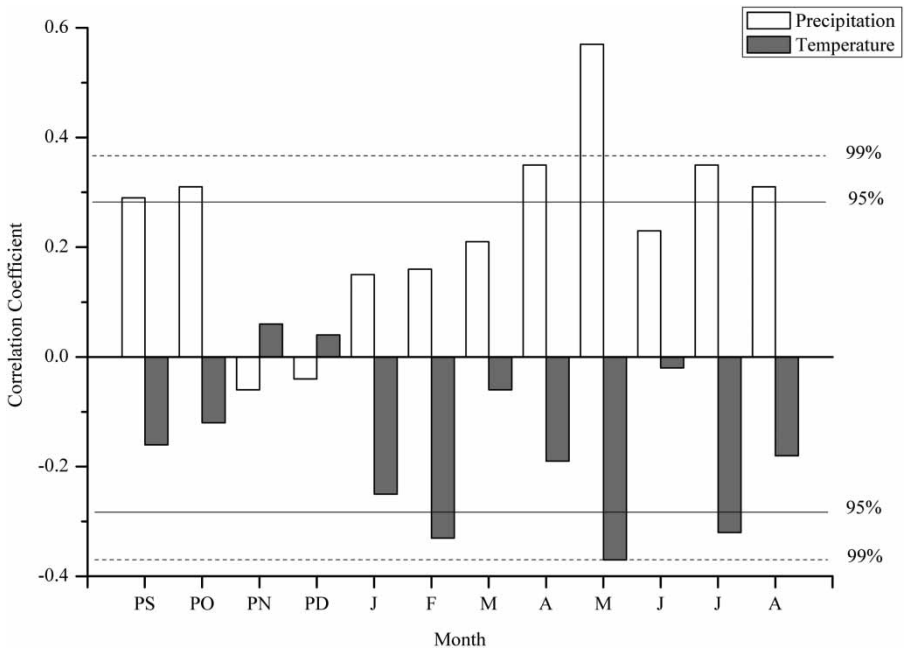

Figure 4 | Correlation coefficient between PC1 and the monthly climate.

Table 5 | Statistics of calibration and verification test results

Calibration			Verification				
Time span	**R**	**R^2**	**Time span**	**r**	**RE**	**CE**	**ST**
1969–1989	0.71**	0.50	1990–2013	0.64**	0.40	0.41	16+/5−*
1990–2013	0.56*	0.31	1969–1989	0.71**	0.36	0.35	17+/5−*
1969–2013	0.62**	0.38					

r, Pearson's correlation coefficient; R^2, explained variance; RE, reduction of error; CE, coefficient of efficiency; ST, sign test.
*Denotes significance at $p(a) < 0.05$.
**Denotes significance at $p(a) < 0.01$.

1977–1989. Dry periods (lasted longer than 11 years) were 1567–1597, 1604–1614, 1641–1656, 1684–1700, 1734–1755, 1817–1830, 1913–1932, 1953–1971, and 1990–2005. The longest wet period is 1701–1733 (33 years) and the longest dry period is 1567–1597 (31 years).

Spectral analysis

The statistical parameters of the IMF components are shown in Figure 7 and Table 7. IMF 1 and IMF 2 were significantly correlated with our reconstruction and were the major components. The amplitudes of IMF 1 and IMF 2 were very high. The secondary components were IMF 3, IMF 4, and IMF 5. In contrast, there was no statistically significant correlation with IMF 6. The major periodic oscillations of IMF 1–IMF 5 were about 2–5 years (IMF 1), 6–10 years (IMF 2), 11–18 years (IMF 3), 28–60 years (IMF 4), and 90–120 years (IMF 5). The 2–5 year cycle may relate to the quasi-biennial and Southern Oscillations influenced by alternating east- and west-wind regimes in the equatorial stratosphere lasting 26–30 months (Naujokat 1986). The 6–10 year cycle may be associated with El Niño–Southern Oscillation (ENSO) variability (Allan

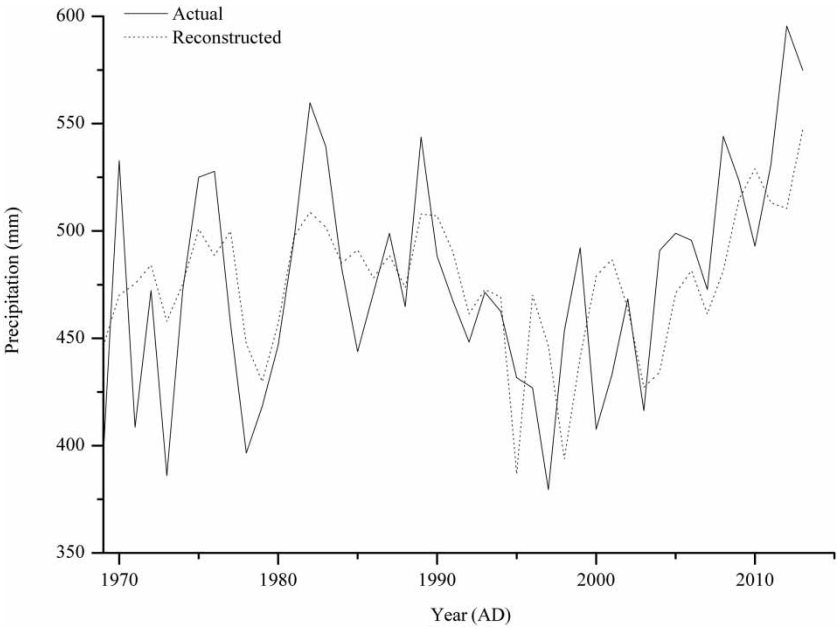

Figure 5 | Comparison of meteorological measurement and reconstructed precipitation from 1969 to 2013.

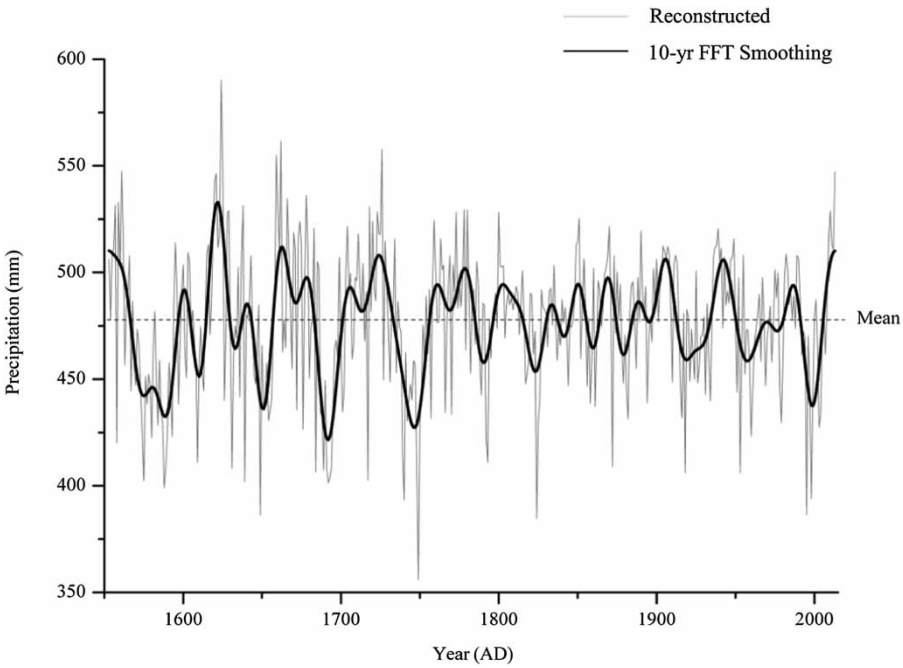

Figure 6 | Reconstructed 461-year precipitation and its 10-year FFT smoothing.

et al. 1996). Moreover, IMF 4 showed relatively stable oscillation on 28–60 years cycle. Larger fluctuations are seen at the front and back of our reconstruction. The IMF5 component revealed the potential for an unstable oscillation on a centennial scale. However, low correlation with our reconstruction suggests that this centennial signal has only a low explanatory power.

Table 6 | Rankings of extremely dry/wet years in the reconstructed series

Rank	Dry year	Precipitation (mm)	Wet year	Precipitation (mm)
1	1749	355.92	1624	590.00
2	1824	384.81	1662	561.50
3	1649	386.25	1726	557.83
4	1995	386.48	1659	554.86
5	1740	393.31	1561	547.49
6	1998	393.99	1625	547.18
7	1588	398.92	2013	547.13
8	1692	401.35	1621	546.32
9	1639	401.78	1620	543.18
10	1575	402.40		
11	1717	402.56		
12	1693	403.77		
13	1953	405.94		
14	1918	406.10		
15	1684	406.43		
16	1748	407.09		
17	1689	407.45		
18	1691	408.06		
19	1589	408.12		
20	1694	408.17		
21	1631	408.26		
22	1872	408.86		

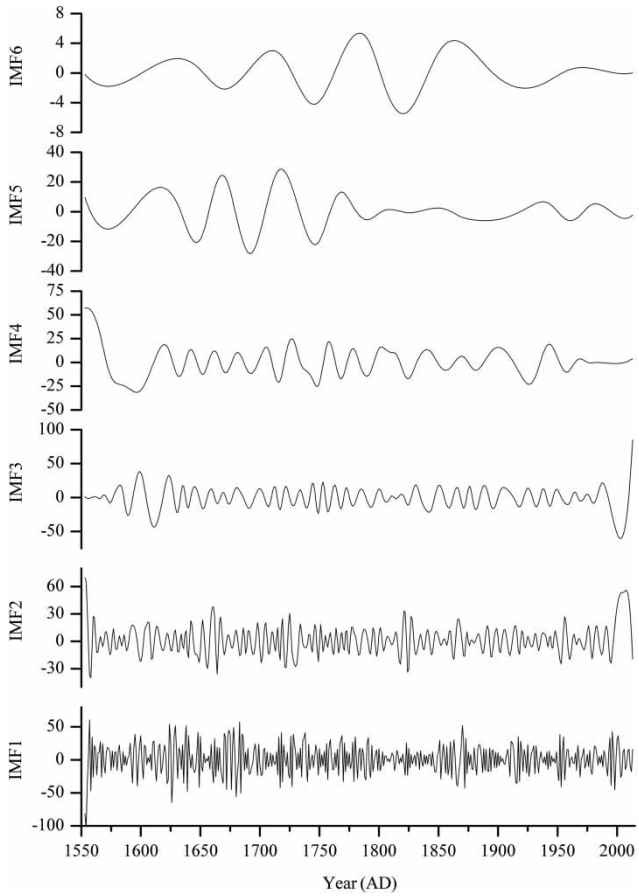

Figure 7 | IMF components of the reconstructed series.

DISCUSSION

Climate–growth relationships

Temperature affects tree growth by influencing soil moisture, plant respiration, and transpiration (Sheppard *et al.* 2004; Wang *et al.* 2008; Fang *et al.* 2010a, 2010b). These effects are exacerbated if precipitation is not adequate during the growing season. This pattern can often be inferred from tree-ring width chronologies that are positively correlated with rainfall and negatively correlated with temperature (Zhang *et al.* 2003; Qin *et al.* 2004; Fan *et al.* 2008). After combining the monthly climate data, the total precipitation from previous September to current August showed high correlations ($r = +0.62$, $p(a) < 0.01$, $n = 45$) with the PC1 of the four chronologies.

Table 7 | The statistical parameters of IMF components

IMF components	IMF1	IMF2	IMF3	IMF4	IMF5	IMF6
Primary period	2–5	6–10	11–18	28–60	90–120	150–180
Correlation coefficient[a]	0.59*	0.35*	0.40*	0.39*	0.14*	0.08

[a]Correlation coefficient between reconstruction and IMF.
*Significance at $p(a) < 0.01$.

Regional comparison

Comparison with the dry/wet events recorded in the history of the southern TRH region from the yearly charts of dryness/wetness in northwest China for the last 500-year period (Bai 2010) shows many extreme wet years (such as 1561, 1624, 1659, and 1726) and dry years (such as 1589,

1649, 1693, 1740, 1749, 1872, 1918, and 1995) in the reconstruction. For instance, there was a serious drought in Zaduo, Zhiduo, and Yushu in 1872 (Wen 2006), which exists in our reconstruction. The Zaqu River in this area was also dry in 1918, and there was a multiyear drought centered on 1995 in the area (Wen 2006).

We compared our reconstruction with three tree-ring chronologies of nearby areas: Delingha (Shao *et al.* 2005), Wulan (Shao *et al.* 2005), and Shenge (Sheppard *et al.* 2004) (Figure 1). Correlation analysis indicated that our reconstruction has strong correlation with tree-ring chronologies from the three areas. The correlation coefficients are 0.65 ($p(a) < 0.01$, $n = 440$), 0.60 ($p(a) < 0.01$, $n = 440$), and 0.63 ($p(a) < 0.01$, $n = 440$), respectively. Figure 8 shows that most dry periods, such as the 1570s–1590s, 1740s–1760s, 1770s–1800s, and 1830s–1840s, coincide with low-growth periods of trees in these regions. Our reconstruction significantly correlates with the precipitation reconstruction of the northeastern Tibetan Plateau (Fang *et al.* 2010a, 2010b) ($r = +0.68$, $p(a) < 0.01$, $n = 454$) and the drought reconstruction of the southeastern Tibetan Plateau (Yang *et al.* 2014) ($r = +0.66$, $p(a) < 0.01$, $n = 454$). The correlations between smoothed reconstruction (apply an 11-year moving average) and these two smoothed reconstructions (apply an 11-year moving average) become even higher, the correlation coefficient is 0.71 ($p(a) < 0.01$, $n = 40$) and 0.69 ($p(a) < 0.01$, $n = 40$), respectively. As shown in Figure 9, the peaks and troughs in these reconstructions lines match closely. These three areas share the same drought (1600s–1610s and 1680s–1700s) on an interannual scale. Dry periods (1690s–1700s and 1740s–1750s) are also consistent with the drought index reconstruction

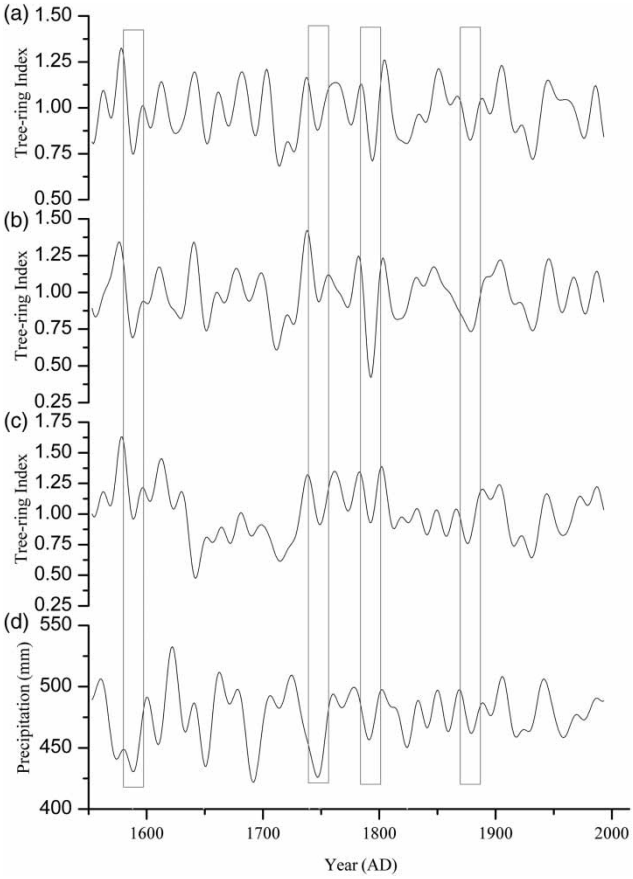

Figure 8 | Comparison of 11-year low-pass filter between our reconstructed series (d) and other tree-ring chronologies from Delingha (a), Wulan (b), and Shenge (c).

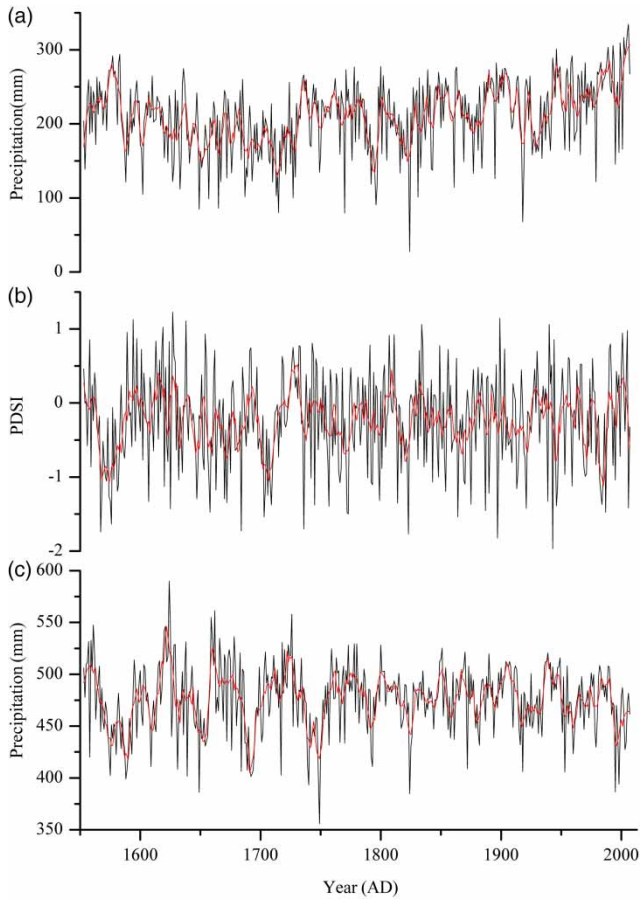

Figure 9 | Comparison of the reconstruction series from different areas: (a) the precipitation reconstruction of the northeastern Tibetan Plateau, (b) the drought reconstruction of the southeastern Tibetan Plateau, (c) our reconstruction precipitation (locations for the regions in Figure 1).

for Zaduo in Qinghai Province, China (Shi *et al.* 2009). Droughts during the 1950s–1970s period also occurred in the precipitation reconstruction of the northeastern Tibetan Plateau (Liu *et al.* 2006a). The 1604–1614 and 1641–1656 droughts were also widespread in northwest China. These 17th century droughts are also reported in northeastern and southeastern Tibetan Plateau (Liu *et al.* 2006a, 2006b; Gou *et al.* 2013; Yang *et al.* 2014). The 1684–1700 drought was also reported in tree-ring width or oxygen isotope reconstructed precipitation in the Qaidam Basin (Zhang *et al.* 2003; Wang *et al.* 2013), and streamflow reconstructions for the Kherlen River (Davi *et al.* 2013) and the Selenge River (Davi *et al.* 2006) in Mongolia. Moreover, we compared our reconstruction with the MADA (Monsoon Asia Drought Atlas) (Cook *et al.* 2010) dataset in the public section (1553–2005) of corresponding grid point dataset (33.75°N, 96.25°E) (Figure 10). Correlation analyses between our reconstruction and MADA were performed from June to August. The correlation coefficients are 0.66 ($p(a) < 0.01$, $n = 452$); this connection suggests a possible link with the interactions between our reconstruction and the monsoon system.

CONCLUSIONS

A precipitation reconstruction of the southern TRH region was performed for 1553–2013 based on the tree-ring width chronology of juniper. We established a model between the PC1 of the four chronologies and total precipitation for the interval from September to August. Our reconstruction revealed nine dry and ten wet periods during the past 461 years. Comparison of our reconstructions with tree-ring chronologies from nearby areas shows that most dry periods coincide with low-growth periods of trees in these regions, and that tree growth is similar throughout this region. Our reconstruction also has wet/dry periods similar to the reconstructions from nearby areas. The EMD analysis suggests the existence of significant periods with intervals of 2–5, 6–10, 11–18, and 28–60 years. Our results are preliminary and require confirmation from ongoing dendroclimatological studies of the southern TRH region. Thus, further work should be undertaken to develop more reliable tree-ring networks, and to explore the possible links between climatic variation reflected in the reconstruction and large-scale climate forcing. Continued work in this direction

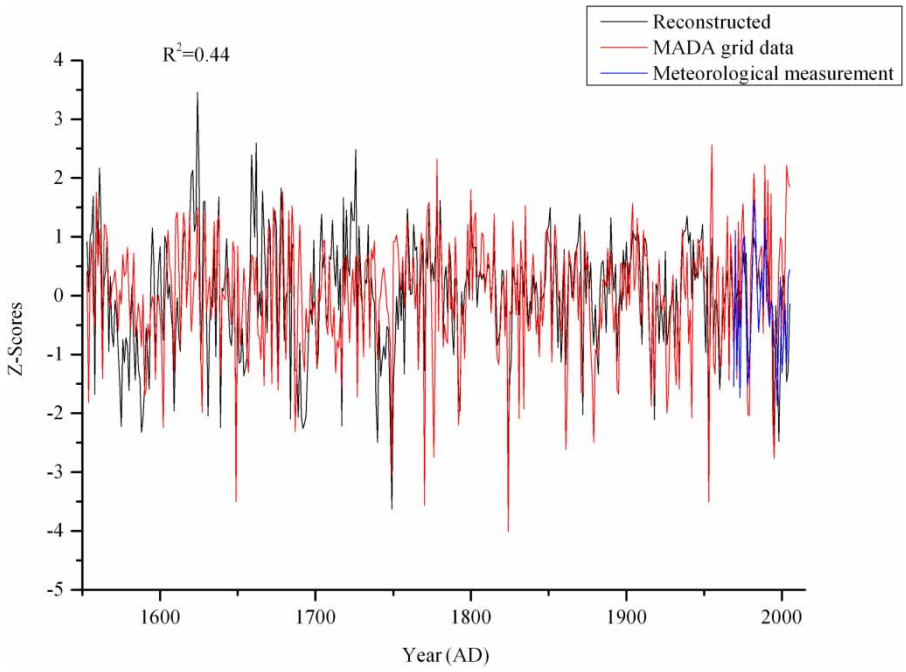

Figure 10 | Comparison of our reconstruction, meteorological measurement, and MADA.

should enable us to understand better the variation characteristics of rainfall and drought in and around the TRH region.

ACKNOWLEDGEMENTS

This research was supported by the National Natural Science Foundation of China (41772173).

REFERENCES

Allan, R., Lindesay, J. & Parker, D. 1996 *El Nino: Southern Oscillation and Climatic Variability*. Australia Press, Melbourne.

Bai, H. Z. 2010 *Yearly Charts of Dryness/Wetness in Northwest China for the Last 500-Year Period*. China Meteorological Press, Beijing (in Chinese).

Bao, G., Liu, Y., Liu, N. & Linderholm, H. W. 2015 Drought variability in eastern Mongolian Plateau and its linkages to the large-scale climate forcing. *Clim. Dyn.* **44** (3–4), 717–733.

Chen, F., Yuan, Y., Yu, S., Zhang, T., Shang, H., Zhang, R., Li, Q. & Fan, Z. 2015 A 225-year long drought reconstruction for east Xinjiang based on Siberia larch (larix sibirica) tree-ring widths: reveals the recent dry trend of the eastern end of Tien Shan. *Quatern. Int.* **358**, 42–47.

Cook, E. R. 1985 *A Time Series Analysis Approach to Tree-Ring Standardization*. *Dissertation*, University of Arizona, Tucson.

Cook, E. R. & Kairiukstis, L. A. 1990 *Methods of Dendrochronology: Applications in the Environmental Science*. Kluwer, Dordrecht.

Cook, E. R., Anchukaitis, K. J., Buckley, B. M., D'Arrigo, R. D., Jacoby, G. C. & Wright, W. E. 2010 Asian monsoon failure and megadrought during the last millennium. *Science* **328** (5977), 486 – 489.

Davi, N. K., Jacoby, G. C., Curtis, A. E. & Baatarbileg, N. 2006 Extension of drought records for central Asia using tree rings: West-central Mongolia. *J. Climat.* **19**, 288–299.

Davi, N. K., Pederson, N., Leland, C., Nachin, B., Suran, B. & Jacoby, G. C. 2013 Is eastern Mongolia drying? A long-term perspective of a multidecadal trend. *Water Resour. Res.* **49**, 151–158.

Fan, Z. X., Bräuning, A. & Cao, K. F. 2008 Tree-ring based drought reconstruction in the central Hengduan Mountains region (China) since AD 1655. *Int. J. Climatol.* **28**, 1879–1887.

Fan, Z. X., Bräuning, A., Yang, B. & Cao, K. F. 2009 Tree-ring density-based summer temperature reconstruction for the central Hengduan Mountain in southern China. *Glob. Planet Change* **65** (1–2), 1–11.

Fang, K., Gou, X., Chen, F., Li, J., D'Arrigo, R., Cook, E., Yang, T. & Davi, N. 2010a Reconstructed droughts for the southeastern Tibetan plateau over the past 568 years and its linkages to the Pacific and Atlantic ocean climate variability. *Clim. Dyn.* **35** (4), 577–585.

Fang, K. Y., Gou, X. H., Peters, K., Li, J. & Zhang, F. 2010b Removing biological trends from tree-ring series: testing modified hugershoff curves. *Tree-Ring Res.* **66** (1), 51–59.

Fritts, H. 1976 *Tree Rings and Climate*. Elsevier, New York.

Fritts, H. 2001 *Tree Rings and Climate*. Blackburn Press, Caldwell, New Jersey.

Gou, X., Chen, F., Cook, E., Jacoby, G., Yang, M. & Li, J. 2007a Streamflow variations of the Yellow River over past 593 years in western China reconstructed from tree rings. *Water Resour. Res.* **43**. doi:10.1029/2006WR 005705.

Gou, X., Chen, F., Jacoby, G., Cook, E., Yang, M., Peng, J. & Zhang, Y. 2007b Rapid tree growth with respect to the last 400 years in response to climate warming, northeastern Tibetan Plateau. *Int. J. Climatol.* **27**, 1497–1503.

Gou, X., Peng, J., Chen, F., Yang, M., Levia, D. F. & Li, J. 2008 A dendrochronological analysis of maximum summer half-year temperature variations over the past 700 years on the northeastern Tibetan Plateau. *Theor. Appl. Climatol.* **93** (3–4), 195–206.

Gou, X. H., Deng, Y., Chen, F. H., Chen, F., Yang, M., Fang, K., Gao, L., Yang, T. & Zhang, F. 2010 Tree ring based streamflow reconstruction for the Upper Yellow River over the past 1234 years. *Chin. Sci. Bull.* **55**, 4179–4186.

Gou, X. H., Yang, T., Gao, L., Yang, D., Yang, M. & Chen, F. 2013 A 457-year reconstruction of precipitation in the southeastern Qinghai-Tibet Plateau. *Chin. Sci. Bull.* **58** (10), 1107–1114.

Gou, X. H., Deng, Y., Chen, F. H., Chen, F., Yang, M., Gao, L., Nesje, A. & Fang, K. 2014a Precipitation variations and possible forcing factors on the Northeastern Tibetan Plateau during the last millennium. *Quat. Res.* **81**, 508–512.

Gou, X. H., Deng, Y., Gao, L., Chen, F., Cook, E., Yang, M. & Zhang, F. 2014b Millennium tree-ring reconstruction of drought variability in the eastern Qilian Mountains, northwest China. *Clim. Dyn.* **45** (7–8), 1761–1770.

Harris, R. B. 2010 Rangeland degradation on the Qinghai-Tibetan plateau: a review of the evidence of its magnitude and causes. *J. Arid. Environ.* **74** (1), 1–12.

He, Y. J. 2008 *Research of Forest Plant Diversity and Protection in the Three-River Source Nature Reserve*. China Forestry Publishing House, Beijing.

Holmes, R. L. 1983 Computer-assisted quality control in tree-ring dating and measurement. *Tree-Ring Bull.* **43**, 69–78.

Huang, N. E., Shen, Z., Long, S. R., Wu, M. C., Shih, H. H. & Zheng, Q. 1998 The empirical mode decomposition and the Hilbert spectrum for nonlinear and non-stationary time series analysis. *Proc. R. Soc. Lond. A* **454A**, 903–995.

Li, J., Chen, F., Cook, E. R., Gou, X. H. & Zhang, Y. 2007 Drought reconstruction for north central China from tree rings: the value of the Palmer drought severity index. *Int. J. Climatol.* **27**, 903–909.

Li, J., Cook, E. R., D'Arrigo, R., Chen, F., Gou, X., Peng, J. & Huang, J. 2008 Common tree growth anomalies over the northeastern Tibetan Plateau during the last six centuries: implications for regional moisture change. *Global Change Biol.* **14** (9), 1096–2107.

Liu, M., Li, D., Luan, X. & Wen, Y. 2005 Ecosystem services and its value evaluation of Sanjinagyuan region. *J. Plant Resour. Environ.* **14** (1), 40–43.

Liu, Y., An, Z., Ma, H., Cai, Q., Liu, Z., Kutzbach, J. K., Shi, J., Song, H., Sun, J., Yi, L., Tang, Y. & Wang, L. 2006a Precipitation variation in the northeastern Tibetan Plateau recorded by the tree rings since 850 AD and its relevance to the Northern Hemisphere temperature. *Sci. China Ser. D* **49** (4), 408–420.

Liu, Y., Yang, Y. K., Cai, Q. F., Ma, H. Z. & Shi, J. F. 2006b June to July runoff reconstruction for Huangshui river from tree ring width of for the last 248 years. *J. Arid Land Resour. Environ.* **20** (6), 69–73.

Meko, D. M. & Graybill, D. A. 1995 Tree-ring reconstruction of Upper Gila River discharge. *Water Resour. Bull.* **31**, 605–616.

Naujokat, B. 1986 An update of the observed Quasi-Biennial Oscillation of stratospheric winds over the tropics. *J. Atmos. Sci.* **43**, 1873–1877.

Qin, N. S., Jin, L. Y., Shi, X. H., Wang, Q. C., Lin, L., Chen, F. & Li, L. M. 2004 A 518-year runoff reconstruction of Tongtian river basin using tree-ring width chronologies. *Acta Geogr. Sin.* **59** (4), 550–556.

Shao, X., Huang, L., Liu, H., Liang, E., Fang, X. & Wang, L. 2005 Reconstruction of precipitation variation from tree rings in recent 1000 years in Delingha, Qinghai. *Sci. China Ser. D Earth Sci.* **48**, 939–949.

Shao, Q. Q., Zhao, Z. P., Liu, J. Y. & Fan, J. W. 2010a The characteristics of land cover and macroscopical ecology changes in the Source Region of Three Rivers in Qinghai-Tibet plateau during last 30 years. In: *Geoscience and Remote Sensing Symposium (IGARSS), 2010 I.E. International, IEEE*.

Shao, Q. Q., Zhao, Z. P., Liu, J. Y. & Fan, J. W. 2010b The characteristics of land cover and macroscopical ecology changes in the source region of three rivers on Qinghai-Tibet Plateau during last 30 years. *Geogr. Res.* **29** (8), 1139–1451.

Shao, X., Xu, Y., Yin, Z. Y., Liang, E., Zhu, H. & Wang, S. 2010c Climatic implications of a 3585-year tree-ring width chronology from the northeastern Qinghai–Tibetan Plateau. *Quat. Sci. Rev.* **29**, 2111–2122.

Sheppard, P., Tarasov, P., Graumlich, O., Sterle, L. H. & Thompson, L. 2004 Annual precipitation since 515BC reconstructed from living and fossil juniper growth of Northeast Qinghai Province, China. *Clim. Dyn.* **23**, 869–881.

Shi, X., Qin, N., Shao, X., Wang, Q., Zhu, X. & Zhu, H. 2009 The drought and flood signals in recent 700 years indicated by long tree-rings of Sabina Tibetica in Zaduo of Qinghai Province. *Plat. Meteor.* **28** (4), 769–776.

Van Loan, C. 1992 *Computational Frameworks for the Fast Fourier Transform*. Society for Industrial and Applied Mathematics, Philadelphia, PA.

Wang, X., Zhang, Q. B., Ma, K. & Xiao, S. 2008 A tree-ring record of 500-year dry-wet changes in northern Tibet, China. *Holocene* **18** (4), 579–588.

Wang, W., Liu, X., Xu, G., Shao, X., Qin, D., Sun, W., An, W. & Zeng, X. 2013 Moisture variations over the past millennium characterized by Qaidam Basin tree-ring $\delta^{18}O$. *Chin. Sci. Bull.* **58**, 3956–3961.

Wen, K. G. 2006 *Chinese Meteorological Disasters Ceremony-Qinghai*. Chinese Meteorological Press, Beijing (in Chinese).

Wigley, T. M., Briffa, K. R. & Jones, P. D. 1984 Average value of correlated time series, with applications in dendroclimatology and hydrometeorology. *J. Clim. Appl. Meteorol.* **23**, 201–234.

Wu, D., Zhao, Y., Pei, Y. & Zhai, J. 2011 Variation trends of temperature and precipitation in Lancang-Mekong River Basin during 1980–2009. *J. China Inst. Water Resour. Hydropower Res.* **9** (4), 304–312.

Yang, B., Qin, C., Wang, J., He, M., Melvin, T., Osborn, T. & Briffa, K. 2014 A 3,500-year tree-ring record of annual precipitation on the northeastern Tibetan Plateau. *Proc. Natl Acad. Sci. USA* **111**, 2903–2908.

Zhang, Q., Cheng, G., Tong, Y., Kang, X. & Huang, J. 2003 A 2,326-year tree-ring record of climate variability on the northeastern Qinghai-Tibetan plateau. *Geophys. Res. Lett.* **30** (14), HLS 2-1.

Zhao, X. Q. & Zhou, H. K. 2005 Eco-environmental degradation, vegetation regeneration and sustainable development in the headwaters of Three Rivers on Tibetan Plateau. *Chin. Sci. Bull.* **20** (6), 471–476.

Zhou, X., Wan, Z. & Du, Q. 1986 *The Vegetation of Qinghai*. Qinghai People's Press, Xining.

First received 22 November 2017; accepted in revised form 8 April 2018. Available online 26 April 2018